Third AO4ELT Conference - Adaptive Optics for Extremely Large Telescopes
Florence, Italy. May 2013
ISBN: 978-88-908876-0-4
DOI: 10.12839/AO4ELT3.13273

FROM CANARY TO E-ELT: LESSONS LEARNED IN OPEN-LOOP TOMOGRAPHY

O. Martin[1a], E. Gendron[1], G. Rousset[1], F. Vidal[1], Morris. T. J[2], Basden A.G.[2], and Myers R.M.[2]

[1] LESIA, Observatoire de Paris, CNRS, UPMC, University Paris-Diderot, 5 place Jules Janssen, 92195 Meudon, France
[2] Centre for advanced Instrumentation, Department of Physics, Durham University, Durham, DH1 3LE, UK

Abstract. CANARY is the on-sky demonstrator of the Multi-Object AO concept for EAGLE, the near-IR AO-compensated multi-object spectrograph proposed for the E-ELT in 2010. The CANARY experiment has been developed to prove the reliability of the open-loop tomographic control and quantify its performance. CANARY has successfully passed this demonstration using three NGSs in 2010 and with additional Rayleigh LGS in 2012 and 2013. We first remind the principle of the MMSE reconstruction used by the Learn&Apply algorithm and then detail some considerations on a tomography strategy for ELT. We then compare the performance of MOAO to SCAO and GLAO, obtained during the last observation runs of Canary in 2012 and 2013.

1 Introduction

One of the future great challenge in infra-red astronomy is the study of the formation and evolution of the first galaxies of the Universe. Thanks to the huge light-collecting power of the Extremely Large Telescopes [1], it will be possible to observe by spectroscopy high redshift galaxies as far as $z \sim 7$. Nevertheless, such a scientific case requires the multiplex observation of many of these objects distributed over a very large field of view (5 to 10 arcmin). Some scientific projects, as EAGLE and EVE [2], could require a few ten of milliarcsec resolution this can be only reached with a large field of view Adaptive Optics system based on Laser Guide Stars to compensate the lack of natural guide stars in such cosmological fields.

Multi-object Adaptive Optics has been created to fulfill these requirements. However, the feasibility and performance of MOAO has to be demonstrated on-sky, especially the open-loop configuration, the tomographic reconstruction and the instrumental calibrations. This is the role of Canary [3] - the technical demonstrator of MOAO - which is set at the William Hershel Telescope. A first on-sky demonstration of MOAO using only NGS has already been led in 2010 [4]. We give in this proceeding an overview of the phase B on-sky results of Canary obtained in 2012 and 2013, using both NGS and Rayleigh LGS.

2 The Canary experiment

The Canary project was started in 2007 and now is set up at the William Hershel Telescope at La Palma. The full demonstration of the feasibility of MOAO, using NGS and LGS in an E-ELT configuration has been split into three phases. The first one (called phase A) has concerned

[a] olivier.martin@obspm.fr

the on-sky validation of MOAO using only three NGS and has been successfully passed in 2010 [4]. Then, we added LGS to the previous setup to get the so-called phase B set-up, that was successfully passed in 2012, using one LGS, and in 2013 using four LGS (see Tim Morris *Multiple Object Adaptive Optics: Mixed NGS/LGS tomography* in this proceeding). Finally, during the phase C (expected for 2014-15), Canary will be designed as a single scientific MOAO channel, with a first closed-loop stage acting as M4 (the adaptive DM of the E-ELT) to compensate the ground turbulent layer, followed by a second stage of pure MOAO.

In order to quantify the on-sky performance of Canary, we are using both a diagnostic Shack-Hartmann sensor - the Truth Sensor (TS) - which is looking at the DM, and an IR camera which delivers images on J (1,28 μm), H (1,67 μm) and K (2,2 μm) bands (see Damien Gratadour *Practical issues with phase diversity for NCPA compensation resolved on the CANARY demonstrator* in this proceeding). Thanks to the TS, we are also able to close the loop in SCAO and compare to the performance of MOAO. We compare with GLAO as well, in order to quantify the impact of the tomographic reconstruction in the global performance.

This tomographic reconstruction is performed thanks to the Learn&Apply algorithm [6] based on a Minimum Mean Square Error (MMSE) reconstruction of the on-axis WFS slopes. This algorithm is split into two steps: the first one is an identification step of the turbulent profile and some calibration parameters. Then, thanks to this identification and a model of the spatial covariance of the turbulence, we are able to compute the MMSE reconstructor to be applied on the off-axis measurements [7].

3 Tomographic reconstruction using the Learn&Apply algorithm

3.1 MMSE reconstruction

We remind here the principle of the MMSE reconstruction. In general, the MMSE reconstructor R_{mmse} is applied to off-axis measurements in order to retrieve the phase in the turbulent volume or in a given direction. Instead with Canary, we have chosen to retrieve the on-axis measurements that the TS would measure, which allows us to manage the calibration of the deviations parameters (sensitivity of the WFS, shifting or magnification of the pupil and rotating) by taking the real TS measurements as reference. The tomographic procedure has to minimize the tomographic error that is defined as:

$$\sigma^2_{tomo} = \mathbb{E}\left[||\mathbf{TS} - R_{mmse}.\mathbf{OffAxis}||^2\right], \tag{1}$$

with **OffAxis** the vector of the off-axis measurements and **TS** the TS ones, both of them including turbulence and noise. Minimizing the tomographic error leads to:

$$R_{mmse} = \mathbb{E}\left[\mathbf{TS}.\mathbf{OffAxis}\right]\mathbb{E}\left[\mathbf{OffAxis}.\mathbf{OffAxis}\right]^{-1}. \tag{2}$$

The MMSE reconstructor is computed from two spatial covariance matrices. However, we can not get directly these two matrices from the off-axis measurements. Firstly, we need matrices without statistical fluctuations [7] and secondly we have to be able to perform the tomographic reconstruction without any information from the TS. That's why we need to determine these two matrices from the off-axis measurements only, and this is performed by the Learn&Apply algorithm.

With this algorithm, we first identify the covariance of the noise directly from the measurements, assuming the noise is a white one (spatial and temporal) and decorrelated from any other process. Note that this last assumption can be reviewed for the elongated LGS case. The variance of the noise for each slope is retrieved from a parabolic fitting of the three first samples of the temporal auto-covariance function, that allows to split the variance into a turbulent part and a noise part. This procedure is repeated for each slope - TS included.

Then, we have a model of the spatial covariance matrix of the turbulence - aliasing included - that depends on several parameters like the distribution of the energy of the turbulence in altitude ($C_n^2(h)$ profile), the outer scale, the geometry of NGS and LGS distance and several calibration parameters. The main idea of the L&A algorithm is to identify these parameters on the on-sky measurements from a least-squares fitting procedure, that minimizes the distance between the covariance matrices of our measurements, and produced by our model. Then from this minimization, we get the set of optimal parameters which allows us to describe the tomographic problem and to compute the two required matrices in Eq. 2. The model of the spatial covariance matrix we use is described in [7].

3.2 Computing power required for ELT

One of our concern is the computation time of the reconstructor. Indeed, because of the non-stationnarity of the turbulence - especially the fast variation of the strength of the ground layer-we need to perform the computation as fast as possible. There is a kind a trade-off between the accuracy of the spatial covariance model and the time required to compute the covariance matrix. This is raising the following question: how does the previous computation apply to an ELT ?

We have identified a simple approximated relation between the computation time of a covariance matrix and the number of layers, the number of slopes and the computing power using our model as follow:

$$t_c \simeq 0.0013 * \frac{n_{layers}.n_{slopes}}{P_c\,(\text{GFlops})} \quad \text{(seconds).} \tag{3}$$

From such relation, we can estimate the computing power required to perform the computation of the covariance matrix using our model on an ELT. We start with a 30 layers profile and a 5 NGS 64x54 WFS and 6 LGS 84x84 configuration (EAGLE configuration in phase A) that leads to approximately 63000 slopes (without considering masked sub-apertures by the central obstruction and the corner of the pupil). If we want to perform this computation in less than one minute, we need a computation power of:

$$P_c \simeq 0.0013 * \frac{30 * 63000}{60} = 40\,\text{GFlops.} \tag{4}$$

Note that the full identification will require a much great computing power to be performed quickly. Particularly, if such an algorithm were required on ELT, we would be confronted to allocation in memory and implementation issues of the fitting procedure. Tomography on ELT will probably require smart implementation method to be performed properly, nevertheless novels ideas developed for the RTC implementation can be relevant for such issues (see Damien Gratadour *"Building a reliable, scalable and affordable RTC for ELTs AO instruments* in this proceeding). A first identification of the required parameters of our spatial covariance model can also be performed using an external profiler in order to strongly decrease the time required to perform the identification (see James Osborn *"Stereo SCIDAR: Profiling atmospheric optical turbulence with improved altitude resolution" in this proceeding*).

3.3 New on-sky tomographic strategy

We have processed most of the Canary data sets of WFS synchronized slopes in order to quantify the variability of the on-sky observation conditions. One of the conclusion is that the variation of the global strength of the turbulence is mainly due to the fluctuations of the ground layer strength. We show in Fig. 1 histograms of the seeing at the ground and in altitude computed from more than 4,000 data sets acquired by Canary during the phase B observation runs. The median seeing of the turbulence measured by Canary is equal to 0.695" (0.7" announced by the ING measured using the DIMM) with a median ground seeing of 0.605" and a median altitude seeing of 0.223". The altitude seeing is also much more stable - in terms of strength - than the ground seeing with a rms variation of 0.09" contrary to 0.32" for the ground seeing. Moreover, the altitude turbulence is globally faster than the ground layer with a median wind speed of 5 m/s against 3 m/s for the ground layer. Histograms of the wind speed are shown in Fig. 1.

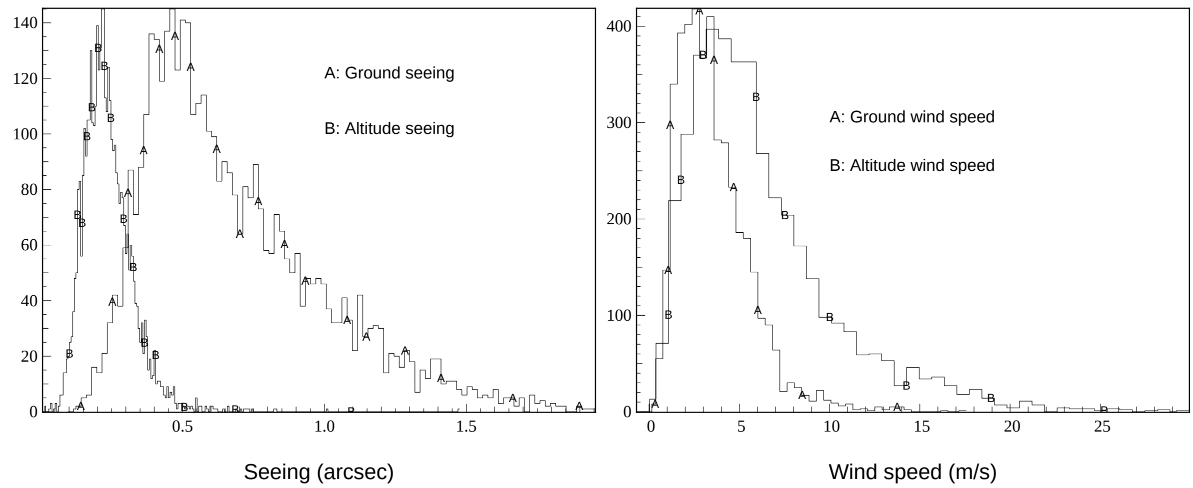

Fig. 1. Left: Histograms of the ground seeing and altitude seeing computed from more than 4000 data sets of WFS synchronized slopes acquired by Canary during the phase B observation runs. **Right:** Histograms of the ground and altitude wind speed computed from the same data sets.

As we seen previously, the computation of the reconstructor may require an expensive computing power if we need to determine the tomographic reconstructor quickly. In order to track the profile variations, we can imagine another strategy, considering that the altitude seeing remains nearly constant compared to the variation of the ground layer strength. Then we could only update the reconstructor by rescaling the ground layer strength only. From an initial full identification of the turbulent profile, we are able to acquire a short data set of WFS synchronized slopes of few tens of seconds in order to estimate the noise, the r_0 and the outer scale. Then, the idea is to use the same parameters retrieved during the full identification of the turbulent profile, rescale all the altitude layers from the airmass, and modify the ground layer strength according to:

$$C_n^2(h=0, t=t_k) = C_n^2(h=0, t=t_0) * \left(\frac{r_0(t=t_k)}{r_0(t=t_0)}\right)^{-5/3.}, \quad (5)$$

with t_0 the time of the full identification of the turbulent profile, t_k the time of the k^{th} updating and $C_n^2(h,t)$ the distribution of the variance of the turbulence in altitude and time.

We report in Fig. 2 the results of an on-sky test of the rescaling procedure. On this example, the rescaling strategy did not allow us to gain in performance in a range of test time of 30 minutes, but allowed us to slightly decrease the fluctuations of the Strehl ratio as function of the r_0 (3.6 % of rms fluctuation against 4.5 % without rescaling). This shows the feasibility of this method. In order to complement this very first on-sky attempt, a finest processing on the open-loop Canary data sets will be required to quantify more precisely the impact on this tomographic strategy on tomographic performance and computing power cost on a greater time range of observation.

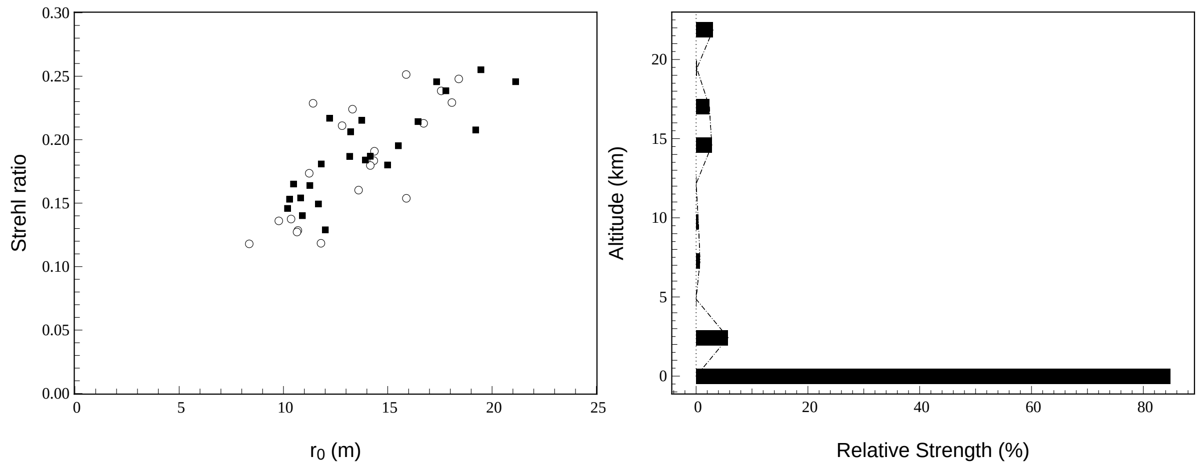

Fig. 2. Left: Strehl ratios as function of the r_0 during the tests of the rescaling tomographic strategy on-sky with Canary. Circles represent MOAO (using 4 LGS and 3 NGS) keeping the same initial reconstructor during 30 minutes and full squares are MOAO using a profile rescaling. **Right:** Turbulent profile identified before the beginning of the on-sky tests of rescaling.

4 On-sky results with LGS

4.1 Impact of the tomography on final on-sky performance

We describe here the results we have accumulated in 2013 on the capability of MOAO using 3 NGS and 4 LGS focused at 21 km. In Fig. 3, we have reported the performance in SCAO, MOAO and GLAO as function of the r_0. These results have been acquired in September 2013 on a same asterism and highlight the impact of the tomographic reconstruction on the final performance. In Sect. 3.3, we have shown the dominance of the ground layer over the altitude layers, which should lead to similar performance between MOAO and GLAO. Nevertheless, the tomographic reconstruction of the weak altitude layers allows to improve significantly the performance of the correction of the wavefront. The identification of the turbulent profile allows to strongly decrease the scattering of the performance as well, which leads to a more optimal and robust command law against variations of the observation conditions, if we are able to pay the price required to the implementation of the tomographic reconstruction.

We have reported in Fig. 4 H-band images of a double star acquired by Canary in 2013 in open-loop, SCAO, MOAO and GLAO using 2 NGS and 4 LGS. These images are an average of thirty images of one second exposure acquired in very comparable observation conditions. When we are running the AO system, we are able to resolve the companion of the binary and

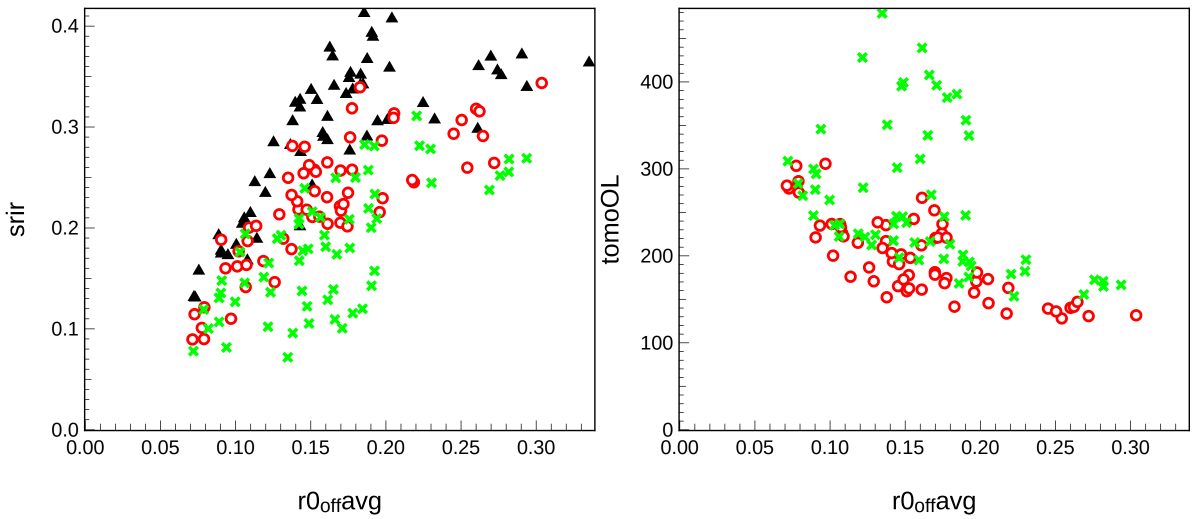

Fig. 3. Left: Strehl ratios in H-band measured on-sky in SCAO (triangles), MOAO (circles) and GLAO (crosses) as function of the r_0. **Right:** Sum of tomographic error and open-loop error in MOAO (circles) and GLAO (crosses) as function of the r_0. These results have been acquired by Canary in September 2013 using three NGS and four LGS.

the most important is to notice that MOAO allows to reach a very comparable resolution power than SCAO and better than GLAO.

Nevertheless, GLAO performance are still quite good compared to what we can do in MOAO, especially because the ground layer is much stronger as it can be expected in simulation for ELTs. During all the observation run of Canary for now, GLAO has always allows us to reach acceptable performance, although worse than MOAO ones, and this technique could be considered as a reliable wide-field AO technique for ELTs in terms of on-sky performance, required resources and scalability as well as tomographic AO techniques.

4.2 Impact of the LGS on the final performance

In Fig. 5, we have reported Strehl ratios and tomographic errors between MOAO using 3 NGS and 4 LGS and 3 NGS only. Although the turbulent profile is essentially at the ground, the LGS help to better reconstruct the on-axis wavefront. LGS can provide a reliable tomographic information but with 3 NGS, the tomographic problem is quite constraint and the impact of the LGS can be less impressive than expected. More results and fine analysis will be provided in future paper on the Canary phase B results.

5 Conclusions

MOAO is a wide-field adaptive optics technique that has been developed in order to fulfill the requirements of a multi-object integral field spectrograph on ELTs. In order to demonstrate the feasibility of MOAO on-sky, the technical demonstrator Canary has been set up at the William Hershel Telescope at La Palma. Since 2010, we have demonstrated the capability of MOAO using both NGS and Rayleigh LGS and the performance of the mixed NGS/LGS tomographic reconstruction using the Learn&Apply algorithm. MOAO is mandatory for multi-objects spectroscopy on faint galaxies on ELTs and the future results of Canary will give a determinant information for the implementation of MOAO at an ELT.

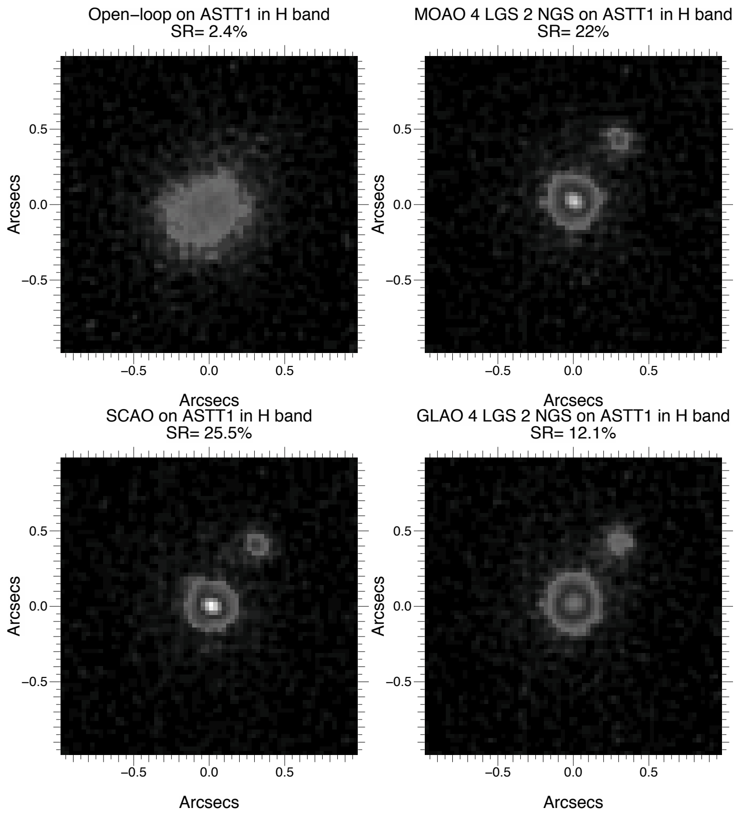

Fig. 4. H-band images of a binary star in Open-loop - MOAO - SCAO and GLAO on the same object and with similar observation conditions acquired in 2013.

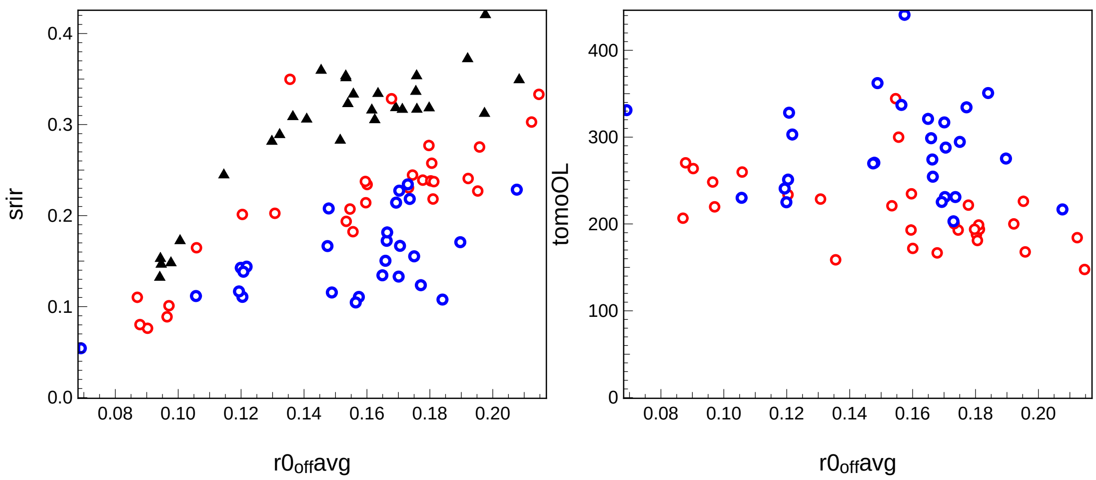

Fig. 5. Left: Strehl ratios in H-band measured on-sky in SCAO (triangles), MOAO using 4 LGS and 3 NGS (red circles) and MOAO using only 3 NGS (blue circles) as function of the r_0. **Right:** Tomographic error plus open-loop error in MOAO 4 LGS and 3 NGS (red circles) and MOAO using only 3 NGS (blue circles) as function of the r_0. These results have been acquired by Canary in September 2013.

This work is supported by CNRS, INSU, Observatoire de Paris, University Paris Diderot-Paris 7, Ecole Normale Superieure de Cachan and European Commission Framework Programme (OPTICON JRA1 Grant 226604, 2009).

References

1. Cuby, J.-G., ”The European ELT: status report”, proc SF2A 2010, 2010.
2. Evans, C.-J., Barbuy, B., Bonifacio, P. *et al.*, ”Multi-object Spectroscopy with the European ELT: Scientific synergies between EAGLE & EVE” in *Ground-based and Airborne Telescopes IV*, proc SPIE 2012, 2012
3. Myers, R. M., Hubert, Z., Morris, T. J. *et al.*, ”CANARY: the On-sky NGS/LGS MOAO demonstrator for EAGLE” in *Adaptive Optics System* , proc SPIE 7015, 2008
4. Gendron, E., Vidal, F., Brangier, M. *et al.*, ”MOAO first on-sky demonstration with CANARY” in Astron.Astrphys 529, pp. L2+, 2011
5. Morris, T.J., Basden, A.-G., Vidal, F. *et al.*, ”Tests of open-loop LGS Tomography with Canary” in *Adaptive Optics System III*, proc SPIE 8447, 2012
6. Vidal, F., Gendron, E., Rousset, G., ”Tomography approach for multi-object adaptive optics” JOSA A 27, pp. A253-A264, November 2010
7. Martin, O., Gendron, E., Rousset ,G., ”Temporal convergence of phase covariance matrix measurements in tomographic adaptive optics” in *Adaptive Optics System III*, proc SPIE 8447, 2012